Utrecht University

Institute for Subatomic Physics

Bachelor thesis

Efficiency study for the reconstruction of charged D^* in pp collisions at 7 TeV at ALICE

Author:
Tim Koreman
4128648

Supervisors:
Dr. Alessandro Grelli
Dr. André Mischke

January, 2017

Abstract

In particle physics determining the efficiency is an important step in measuring the invariant mass of a particle. This thesis presents the study of the efficiency for charged D^* mesons in pp collisions at 7 TeV at ALICE. Specifically this thesis looks at the difference in efficiency between charged D^* mesons being directly created and charged D^* mesons created in B meson decay.

In the lower p_T region, the efficiency is higher for the D^{*+} from beauty compared to D^{*+} from charm. The difference mainly arrises in the vertexing step. We also look at 5 different cuts which differ in the reconstruction method, the effect of these 5 cuts on the ratio between the efficiency for D^{*+} from beauty and from charm is found to be small.

'Have you guessed the riddle yet?' the Hatter said, turning to Alice again.

'No, I give it up', Alice replied: 'what's the answer?'

'I haven't the slightest idea', said the Hatter.

- Lewis Carroll, *Alice in Wonderland*

Contents

1 Introduction

1.1 Theorectical background

Particle physics is the branch of physics that focuses on finding a single model to account for all particle phenomena. The best model constructed thus far is the Standard Model (SM). The SM is an effort to unify all the fundamental forces found in in nature in one model and to account for all the known subatomic particles. In the SM, there are four fundamental forces, which are mediated by their respective gauge bosons. there are the nuclear weak force carried by the W and Z bosons, the nuclear strong force carried by the gluon, the electromagnetic force carried by the photon and gravity carried by the graviton. All of these gauge bosons have been experimentally observed except for the graviton.

In this thesis, the focus has been made on the nuclear strong force, which is described by a theory called Quantum Chromodynamics (QCD). QCD is the theory which describes the interaction between quarks and gluons. Quarks are the particles, which make up hadrons and the strong force is the force that keeps these hadrons from falling apart. There are 2 types of hadrons, baryons and mesons, where baryons consist of 3 quarks, the best known of which are the proton and the neutron, and mesons consist of 1 quark and 1 anti-quark. In QCD, quarks and gluons have a quantum number called color charge, which can have 3 states, namely Red, Green and Blue. Anti-particles can have color charge anti-green, anti-blue or anti-red. A hadron is said to have neutral color charge if it consists of quarks of the three different colors (baryons) or of a color and the same anti-color (mesons). One of the implications from QCD is that hadrons can only exist if they have a neutral color charge, one of the implications this has is that quarks cannot be studied on their own.

There is however a state in which quarks can exist on their own called a Quark-gluon Plasma (QGP). This state of matter exists only a very high temperature and/or very high temperature (see figure 1 for an indication). When the QGP cools down the quarks get back together as hadrons in a process called hadronisation. These hadrons then leave the QGP in hadronic jets.

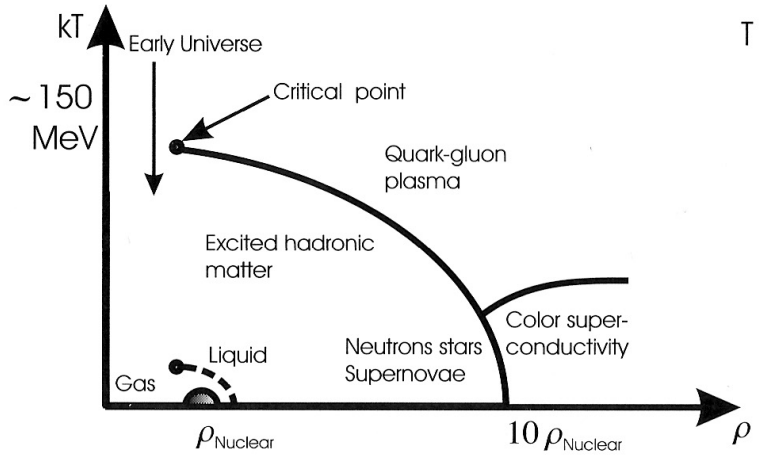

Figure 1: *Phase diagram for hadronic matter. Source: [1].*

One of the reasons to study QGP is to know more about the first phases of our universe. In the first few hundred microseconds after the big bang all the matter, which makes up our universe where in a QGP. So to know more about these first phases of our universe we want to know more about QGP. Another reason to study QGP is to test predictions made by perturbative QCD.

1.2 Motivation

We want to study the properties of QGP, to produce a QGP at the LHC we collide ^{208}Pb nuclei at very high energy (in the order of several TeV). The QGP exists for about 3.3×10^{-7} s [2], which is too short to directly study it so we look for particles produced in the QGP, that can be used as probes. There are many particles, that could be used as probes but there are a few constraints, we want to study the QGP in which they were produced so the probes have to have a strong interaction, which excludes leptons. Hadrons in the QGP lose energy via 2 mechanisms, through collisions and through gluon radiation. Predictions from theory say that the more massive hadrons lose less energy due to radiation and therefore we can say more about what happened with that particle in the QGP. Top quarks have a very short lifetime so they mostly decay before hadronisation takes place so the baryons we want to look for consist of bottom and charm quarks, the most probable baryons with these quarks to be produced are D and B mesons.

At a Pb-Pb collision many paritcles are created which gives many events to reconstruct (see figure 2 for an indication). To be able to say something about the QGP using these probes we need to study the production of these mesons in a more controlled environment, therefore we measure pp collisions. We then compare the two types of collisions assuming we use the same parameters for both types (same energy per nucleon/same magnetic field/etc.). We can then say something about the effect of the QGP on the production of those hadrons.

If the QGP has no effect on the production of hadrons the results from pp collisions should be the same as Pb-Pb collisions (up to a normalisation factor to correct for the larger number of hadrons in Pb-Pb collisions), to study this we can use the Nuclear Modification Factor, R_{AA}, which is defined as [3]:

$$R_{AA} = \frac{1}{\langle T_{AA} \rangle} \frac{dN_{AA}/dp_{\mathrm{T}}}{d\sigma_{pp}/dp_{\mathrm{T}}}, \tag{1}$$

which is the amount of a particle produced in Pb-Pb collisions divided by the amount of these particles produced in pp collisions (normalised for the amount of hadrons in the Pb-Pb collisions).

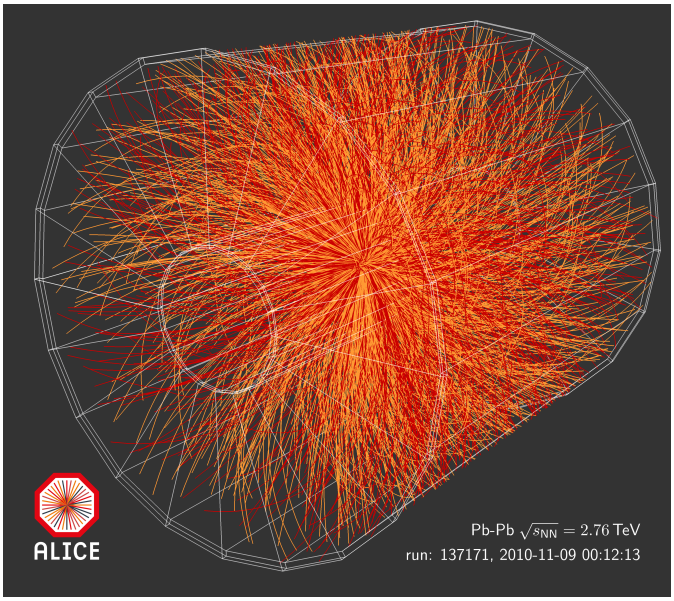

Figure 2: *Eventdisplay of a Pb-Pb collision at 2.76 TeV, recorded at ALICE on September 11, 2010. Source: [4] .*

1.3 D^{*+} mesons

The D^{*+} mesons consists of a charm and a anti-down quark. We look at D^{*+} mesons, which are directly produced in the QGP from a charm and a anti-down quark and at D^{*+} mesons which come from decaying B mesons. The D^{*+} has 3 known decay channels (with their respective branching ratios [5]):

- $D^{*+} \rightarrow D^0\pi^+$ $(67.7 \pm 0.5)\%$
- $D^{*+} \rightarrow D^+\pi^0$ $(30.7 \pm 0.5)\%$
- $D^{*+} \rightarrow D^+\gamma$ $(1.6 \pm 0.4)\%$

Because the first decay channel has the highest branching ratio we focus on that decay. The D^0 that gets produced in that track decays (it has a decay length of 1.3×10^{-4} m [6]) before it reaches the innermost layer of the detector. The D^0 decays into a kaon and a pion so the particles that are most important for the reconstruction of the invariant mass of the D^{*+} are the pion and the kaon.

2 Experimental setup

2.1 ALICE detector

The ALICE experiment is one of the four big experiments situated at the Large Hadron Collider (LHC) at CERN. The ALICE experiment, which is short for A Large Ion Collider Experiment, has been built to study heavy ion collisions. The detector is able to measure charged leptons, charged hadrons and photons over a large p_{T} range.

The ALICE detector consists of a barrel with many sub detectors (see Figure 3). The detectors within the central barrel (which are most important for this study) are, from the center outwards:

- Inner Tracking System (ITS)
- Time Projection Chamber (TPC)
- Transition Radiation Detector (TRD)
- Time of Flight Detector (TOF)
- Photon Spectrometer (PHOS)
- High Momentum Particle Identification Detector (HMPID)

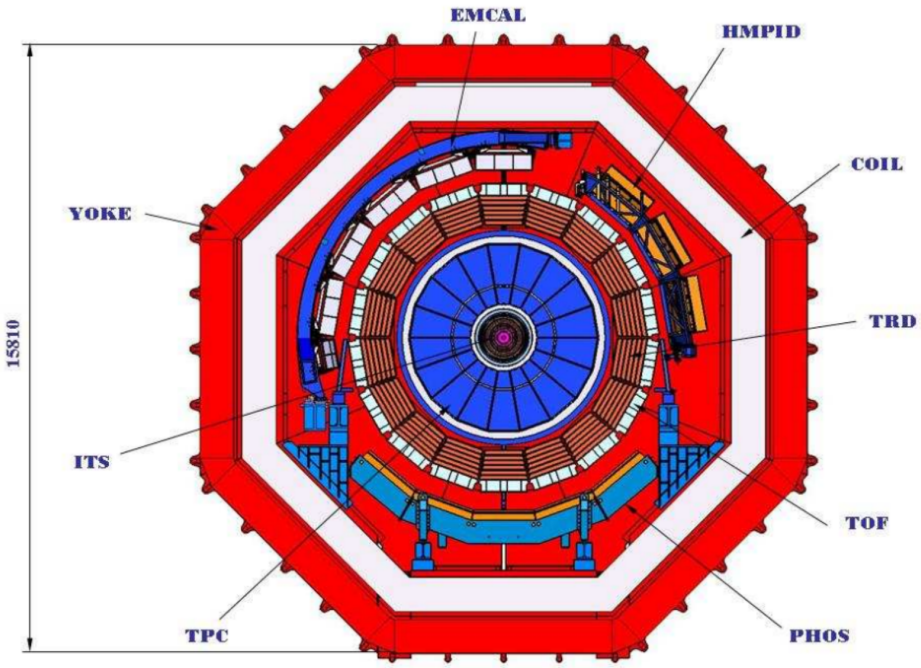

Figure 3: *Vertical slice of the ALICE detector in the xy-plane. In this coordinate system the x axis is perpendicular to the beam line and pointing towards the center of the LHC, the y axis is perpendicular to the x-axis and the beam line. The z axis is in the direction of the beam line so that it forms a right handed coordinate system with the x and y axes. Source: [7].*

All these detectors are placed in a big electromagnet (the red band on Figure 3). For this thesis the ITS, TPC and TOF are the most important so we will look at those in more detail.

The ITS is the innermost detector, it is comprised of six layers of silicon detectors positioned as close as possible to the beam line, the innermost two layers are the Silicon Pixel Detector (SPD), the middle two are the Silicon Drift Detectors (SDD) and the outer two are the Silicon Strip Detector (SSD). The innermost layer is positioned 3.9 cm [8] from the beam line. The ITS can track particles with a high momentum with a very high precision. The ITS is important to construct the primary and secondary vertices. Particles can be identified in the ITS by measuring energy losses.

The TPC is a cylindrically shaped chamber filled with gas (a mixture of neon and carbondioxide [9]). When a charged particle travels through this gas it gives a trail of ionised particles, which can be detected. Using this we can precisely determine the path and the energy loss of a particle. The TPC is the main tracking detector and important in determining the secondary vertex.

The TOF detector is a gas chamber as well used to time the arrival of particles, combining this with the triggers in the ITS gives us a time of flight for a particle which together with its momentum can be used to calculate the mass of the particle.

2.2 Particle identification

One of the most important steps in the event reconstruction is the particle identification. In this step of the reconstruction, after the vertices and the track are reconstructed, it is determined which particles where involved in that event. At ALICE many different techniques are used to identify particles, in this thesis the focus has been made to the techniques to identify charged hadrons, which is the most relevant for this thesis.

The main way charged hadrons are identified is by using the energy loss of the particles in the ITS and the TPC. In the ITS and TPC the particle travels through a medium, silicon and a mixture of neon and carbon dioxide [9] for the ITS and TPC respectively. The charged hadrons travelling through these media cause ionisation in these media. This ionisation leads to loss of energy, this loss of energy can be used to identify particles as shown in figure **??**.

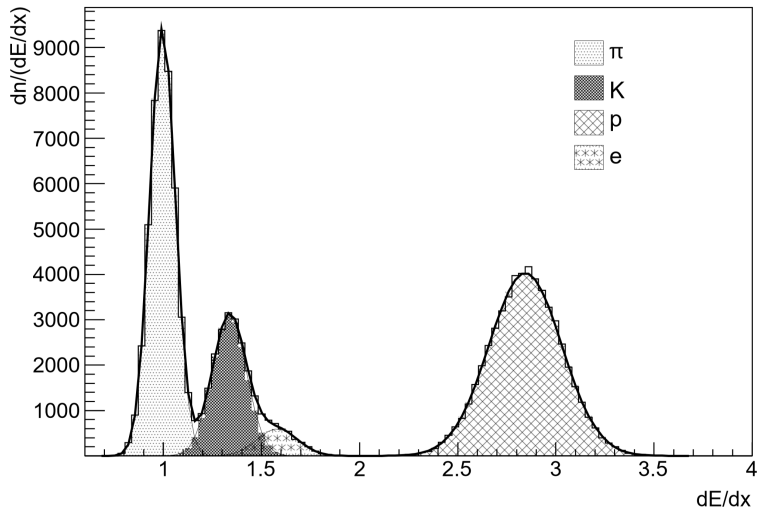

Figure 4: *Simulated dE/Dx distribution for the TPC for electrons, pions, kaons and protons for $p_{\mathrm{T}} = 0.5$ GeV/c showing how this can be used for particle identification. Source: [9].*

2.3 Software

To perform the calculations needed for this thesis the software packages ROOT and AliROOT were used. ROOT is a object oriented-package written in C++ and using C++ as its scripting language. ROOT is specifically made to work with the data generated in particle physics experiments. AliROOT adds libraries specifically to use with the ALICE detector to ROOT.

The starting point of the software written for this thesis was the `DrawEfficiency.cxx` [1] macro from the AliPhysics library. The plots for this thesis were generated in a macro written from scratch, which takes the data from an `AliCFContainer` and use that data to calculate the efficiency for various variables and cut parameters.

2.4 Data used

The data used for this thesis were generated using Monte Carlo simulations. These simulations use the same parameters and conditions as found in the ALICE detector. These simulations simulate 6×10^6 pp-collisions at 7 TeV and then apply the same methods as used for the experimental data to calculate the efficiency.

[1] This macro can be downloaded from the AliPhysics repository [10].

3 Cuts

3.1 Topological cuts

One of the challenges in particle physics is to distinguish data signal from background signal. One of the ways to do this is to apply cuts to the data. Cuts are selection criteria that are being applied to the data. To go from raw data to event identification we apply a series of cuts commonly referred to as a Cut-Flow. These cut values can be varied which will change the signal to noise ratio and the number of identified events, in the most cases cuts that enhance to signal to noise ratio also decrease the number of events. Different cut values also enhance or suppress our D^{*+} signal coming from beauty and from charm quarks differently. We will look in more detail at the topological cuts most important for this thesis.

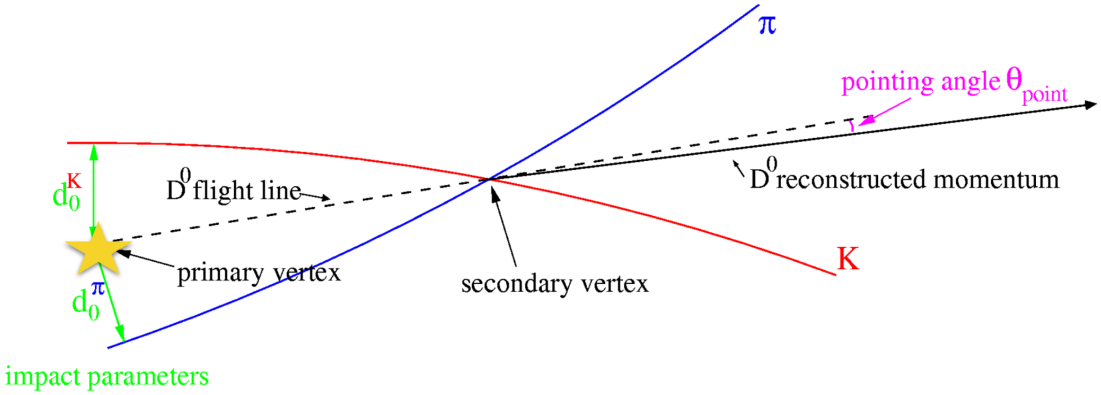

Figure 5: *Diagram of the topology of the events that are being reconstructed for the reconstruction of the* D^{*+} *invariant mass. Source: [3].*

- *DCA:* In the diagram we depict the secondary vertex as being a single point, in reality the pion and the kaon are never measured at the same point due to the finite resolution of the detector. The point they are closest we call the secondary vertex and the distance between the particles at that point is called the distance of closest approach (DCA). For the D^0 meson decay the DCA is expected to be $\sim 200\mu m$ so it can be used as a cut to remove background from the signal.

- $d_0^k \times d_0^\pi$*:* The tracks from the pion and the kaon can te extended, the closest approach for each of the particles to the primary vertex are called the impact parameters (see figure 5). The product of these two impact parameters, d_0^K and d_o^π, can be used as a cut. For random background we expect this product to be a symmetric peak. The pion and the kaon have a difference in mass, the kaon is about four times heavier then the pion. This mass difference leads to a difference in the impact parameters d_0^K and d_0^π. The product of these parameters then gets shifted to one side which means this can be used to make cuts (see figure 6).

- $\cos(\theta_{\text{point}})$*:* From the momentum of the pion and kaon the momentum of the D^0 can be reconstructed. The angle between the reconstructed momentum and the line defined by the primary and secondary vertices is called the pointing angle (θ_{point}). For correct events this angle should be very small so the cosine of this angle should be close to 1 (see figure 7). For random events this angle is evenly distributed so a cut can be made using the cosine of the pointing angle.

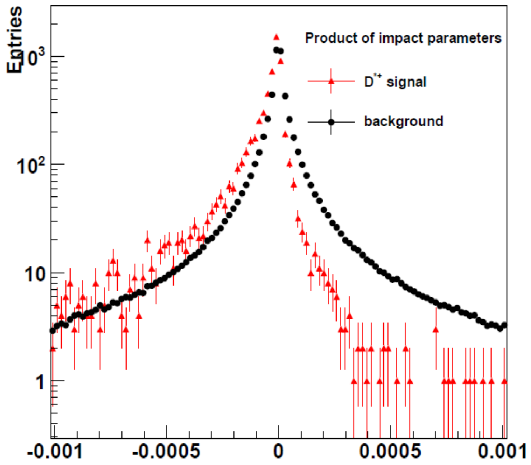

Figure 6: *Product of the impact parameters for montecarlo simulations for* D^{*+} *events. Source: [11].*

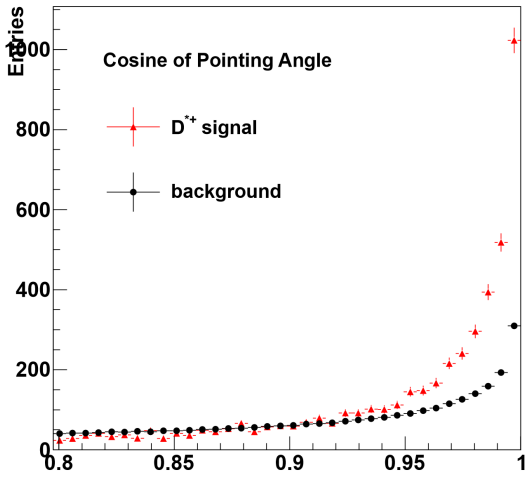

Figure 7: *Cosine of the pointing angle for montecarlo simulations for* D^{*+} *events. Source: [11].*

3.2 Cuts used

We want to study what the effect is of the different reconstruction steps on the ratio between the efficiency between D^{*+} from beauty and D^{*+} from charm. To do this we look at 5 different settings (cuts) for the reconstruction process:

- *Cut 1: No Refit* - For this option no refitting is required which could result in tracks of a lower quality but could possibly lead to interesting tracks that normally would be discarded.
- *Cut 2: 2 Clusters:* - We require a minimum of 2 hits in the ITS.
- *Cut 3: 4 Clusters* - We require a minimum of 4 hits in the ITS.
- *Cut 4: TPC Refit* - For this option we require a TPC refit in addition to the ITS refit.
- *Cut 5: Standard* - The standard option requiring at least 1 hit in the ITS and at least 70 hits in the TPC.

The efficiencies and ratios are calculated for each of these 5 different settings so that comparisons can be made and we can study the effect these settings have on the ratio.

4 Efficiency

At ALICE, one of the goals is to reconstruct the invariant mass of the D^{*+} meson, To do this we want to know the number of D^{*+} produced at a collision. When there is a collision at ALICE a certain number of D^{*+} is measured but there were probably more D^{*+} than measured. During the process from the collision untill the event identification a certain number of D^{*+} mesons is lost, to know how much the efficiency is studied.

To calculate the efficiency we use Monte-Carlo simulations using the same parameters as we have got at ALICE. From this we calculate how much D^{*+} mesons we lose in the process, we do these calculations for different steps in the reconstruction process:

- *Acceptance:* Not all the D^{*+} mesons that are produced in the collision end up in the detector, some fly away in the direction of the beamline. We reject all events with a pseudorapidity of $\eta \geq |0.9|$.

- *Vertexing:* The reconstruction of the primary and secondary vertices starts at the outer layer of the TPC because the track density is minimal there. From these tracks candidate tracks are selected and these tracks are being followed back inwards towards the beamline. Hits along these tracks are being added to the tracking. When the tracking reaches the innermost layer of the TPC the ITS takes over and tries to prolong the tracks as close to the vertex as possible.

  A certain number of hits in the ITS and the TPC is required to correctly reconstruct the vertices. Not all the events pass this process therefore an amount of events is lost in this step.

- *Refitting:* Once the primary and secondary vertices have been reconstructed the track is refitted from the outwards toward the beamline.

- *Reconstruction:* When the primary and secondary vertices have been reconstructed and the refitting has succeeded the event can be reconstructed.

- *Reconstructed Acceptance:* The reconstructed events will be checked to see whether they still are within the acceptance of the detector. Due to the finite resolution of the detector it could be the case that events that where generated within the acceptance now fall outside of the acceptance.

- *Reconstruction ITS:* The reconstructed events have to have a certain number of hits in the ITS, standard there have to be minimally 3 hits in the ITS, 1 of which has to be in the SPD.

- *Reconstruction PPR:* All the cuts are applied to the reconstructed events.

- *Reconstruction PID:* For the reconstructed events data from the TOF is used to identify the particles in the event.

We now look at the efficiency for the D^{*+} production from the charm channel (Figure 8). We can see that the efficiency is highest for the higher p_T bins. When we look at the p_T distribution of the particles (Figure 9) we can however see we have many more particles in the lower p_T bins so we see that the peak in the p_T distribution moves toward the higher p_T bins. The table with the values of the efficiency for each step and each bin has been included in appendix A.

We also look at the efficiency projected onto other variables. These plots have been added in appendix A.

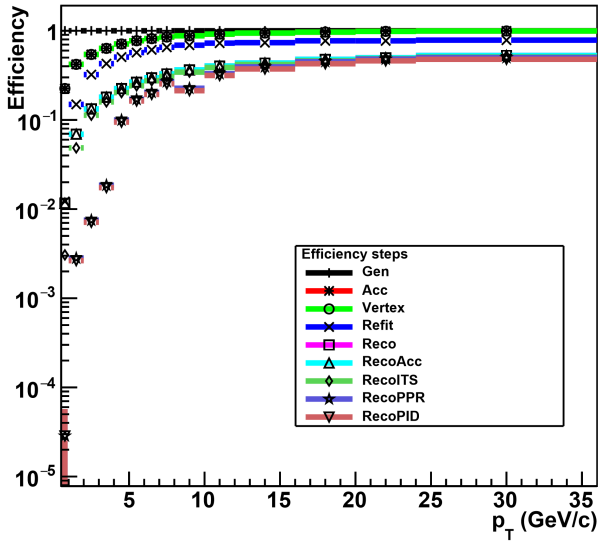

Figure 8: *Efficiency for the reconstruction of* D^{*+} *mesons from the charm channel for the standard* p_{T} *bins and the standard cuts.*

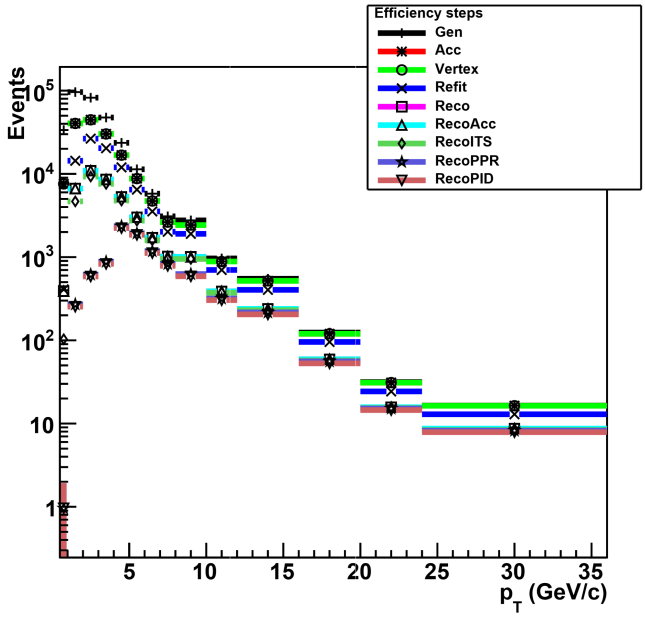

Figure 9: p_{T} *distribution for the reconstruction of* D^{*+} *mesons from the charm channel for the standard* p_{T} *bins and the standard cuts.*

5 Results

The efficiency is different for D^{*+} from charm quarks and D^{*+} from beauty quarks. We can plot the ratio between those two efficiencies. In figure 10, this ratio is plotted for each step and each p_T bin for the standard cuts. For lower p_T it is visible that the efficiency is higher for the D^{*+} from beauty than from charm, in the higher p_T region this difference gets smaller.

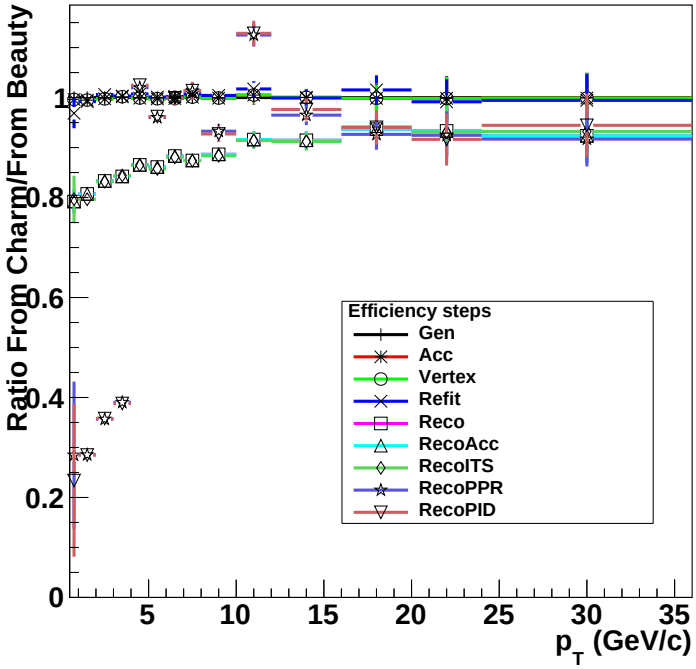

Figure 10: *The ratio between the efficiency for the reconstruction of* D^{*+} *mesons from the charm channel and from the beauty channel for the standard* p_T *bins and the standard cuts.*

We want to look how the ratio between D^{*+} from charm and from beauty varies when we vary the cuts. To do this we look at 4 different cuts, first we look how much they differ from the standard cuts. Then we look how the ratio between D^{*+} from charm and from beauty changes with this difference in cuts. These results are shown in figure 11 and table 1.

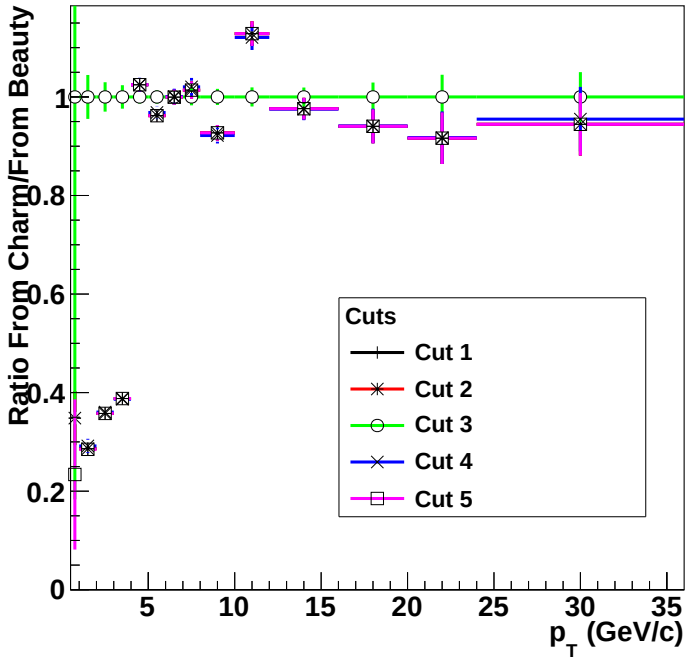

Figure 11: *The ratio between the efficiency for the reconstruction of* D^{*+} *mesons from the charm channel and from the beauty channel for the standard* p_T *bins for 5 different cuts, cut number 5 is the standard cut.*

p_T bins (GeV/c):	Cut 1:	Cut 2:	Cut 3:	Cut 4:	Cut 5:
0.5 - 1	0.35	0.35	1.00	0	0.23
1 - 2	0.29	0.29	1.00	0.29	0.29
2 - 3	0.36	0.36	1.00	0.36	0.36
3 - 4	0.39	0.39	1.00	0.39	0.39
4 - 5	1.02	1.02	1.00	1.02	1.02
5 - 6	0.96	0.96	1.00	0.97	0.96
6 - 7	1.00	1.00	1.00	1.00	1.00
7 - 8	1.01	1.01	1.00	1.02	1.01
8 - 10	0.93	0.93	1.00	0.92	0.93
10 -12	1.13	1.13	1.00	1.12	1.13
12 -16	0.98	0.98	1.00	0.98	0.98
16 - 20	0.94	0.94	1.00	0.94	0.94
20 - 24	0.92	0.92	1.00	0.92	0.92

Table 1: *The ratio between* D^{*+} *from beauty and* D^{*+} *from charm for the 5 different cuts for the standard* p_T *bins.*

6 Discussion

For lower p_T regions figure 10 shows that the efficiency is better for D^{*+} from beauty compared to D^{*+} from charm. This difference mainly comes from the vertexing step. An explanation for this could be that because for the D^{*+} from beauty the B meson first travels its decay length before decaying into a D^{*+} . So when this D^{*+} then decays it is much closer to the ITS then D^{*+} directly formed at the collision. Because of this the D^{*+} from beauty has more hits within the ITS and the TPC which would make it easier to perform the vertexing.

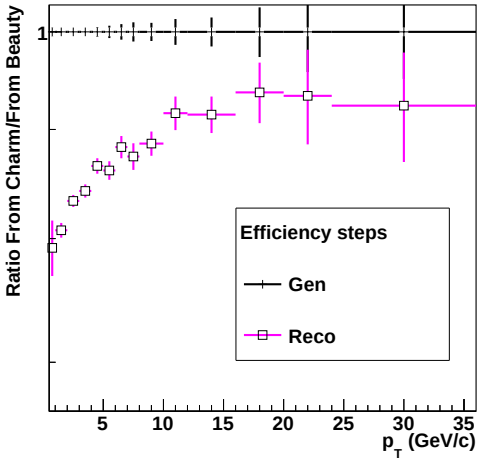

Figure 12: *The ratio between the efficiency for the reconstruction of* D^{*+} *mesons from the charm channel and from the beauty channel for the standard* p_T *bins and the standard cuts between the generation and the reconstruction step.*

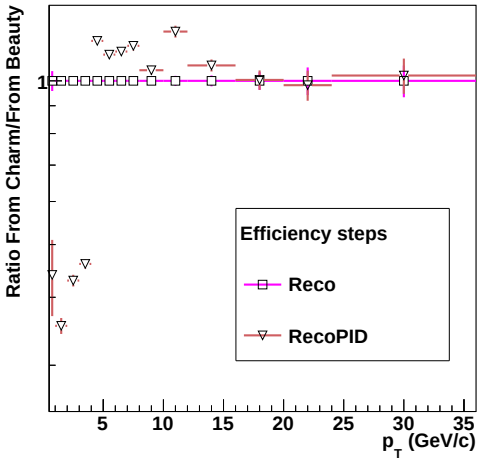

Figure 13: *The ratio between the efficiency for the reconstruction of* D^{*+} *mesons from the charm channel and from the beauty channel for the standard* p_T *bins and the standard cuts between the reconstruction and the particle identification step.*

When we look in more detail at the ratio we can see in figure 12 that we can reconstruct relatively more D^{*+} from beauty than from charm, interestingly we can see in figure 13 that from all the reconstructed events we can identify more of the events from charm than from beauty. So we get more relatively events from beauty but the events we get from charm are of a higher quality.

When we look at figure 11 and table 1 for cut 3 we see that the ratio is 1 for each bin which seems highly unlikely so some sort of error seems likely. For the other 3 cuts there is a clear difference between the efficiency from beauty and from charm but the difference between the cuts is very small, if anything at all. We would expect to see a bigger difference in the ratio between the cuts. In figure 10 we see that the biggest difference between the efficiency from charm and from beauty arises in the vertexing step so we would expect to see that reflected in the ratio. In the results this difference is not visible, this could have multiple reasons. There could be an error in the way the data container was prepared, there could be an error in the data analysis or there could be a physical effect. To determine what was the reason behind the unexpected behaviour more research has to be done.

The data analysis performed for this thesis was done for simulations ran at 7 TeV but at this moment experiments are ran at CERN at 13 TeV. At the time of writing the data for the 13 TeV pp collisions wasn't ready yet for efficiency analysis but the methods used for this analysis at 7 TeV should also be able to be used for the efficiency study at 13 TeV (with minor changes).

7 Conclusion

There is a clear difference between the efficiency for D^{*+} from charm versus D^{*+} from beauty. This difference arrises mainly in the vertexing step. We see that for the D^{*+} from beauty we can reconstruct relatively more tracks but for the D^{*+} from charm we can correctly identify more of the reconstructed tracks. We could conclude that we can reconstruct more events for D^{*+} from beauty but the events we get for D^{*+} from charm are of a higher quality.

The different cuts have a very minimal effect on the ratio between the efficiency for the production of D^{*+} from beauty and from charm. For lower p_{T} bins the efficieny is higher for the D^{*+} from beauty.

References

[1] Ernest M. Henley & Alejandro Garcia, *Subatomic Physics*, World Scientific Publishing, 2007.

[2] P. Foka [ALICE Coll.], *Overview of results from ALICE at the CERN LHC*, J. of Phys.: Conf. Series 455, 012004 (2013).

[3] A. Grelli (2015) *Probing the Quark Gluon Plasma with Heavy Mesons* [presentation slides], Retrieved from `http://www.staff.science.uu.nl/~grell101/StrongInt_TUM_Grelli_27Apr.pdf` on December 20 2016.

[4] CERN Document Server, *ALICE event display of a Pb-Pb collision at 2.76 TeV*, Retrieved from `http://cds.cern.ch/record/2032743` on January 7 2017.

[5] K.A. Olive et al. [Particle Data Group], *Particle Data Group* D^{*+} , Chin. Phys. C38, 090001 (2014).

[6] K.A. Olive et al. [Particle Data Group], *Particle Data Group* D^0, Chin. Phys. C38, 090001 (2014).

[7] H. Gustafsson et al. [ALICE Coll.], *The ALICE experiment at the CERN LHC*, JINST 3, S08002 (2008).

[8] L.Y. Abramova et al. [ALICE Coll.], *Technical Design Report of the Inner Tracking System (ITS)*, CERN/LHCC 99-12 (1999).

[9] G. Dellacasa et al. [ALICE Coll.], *Technical Design Report of the Time Projection Chamber*, CERN/LHCC 2000–001 (2000).

[10] ALIDOC repository, *DrawEfficiency.cxx*, Retrieved from `http://alidoc.cern.ch/AliPhysics/master/_draw_efficiency_8_c.html` on January 7 2017.

[11] P. Kukla, D^{*+} *analysis in proton-proton collisions at* $\sqrt{s} = 2.76$ *TeV using the ALICE detector at CERN*, Master thesis (2011).

Appendices

A Efficiency for other variables (standard cuts)

p_{T}

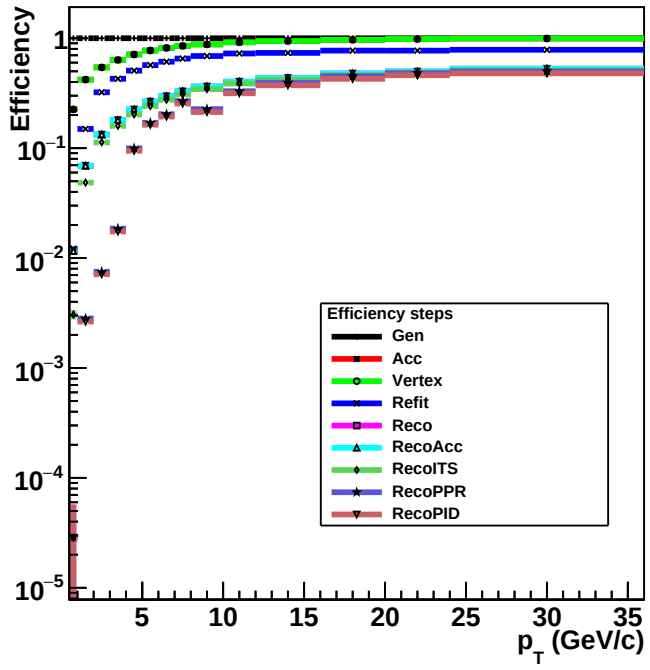

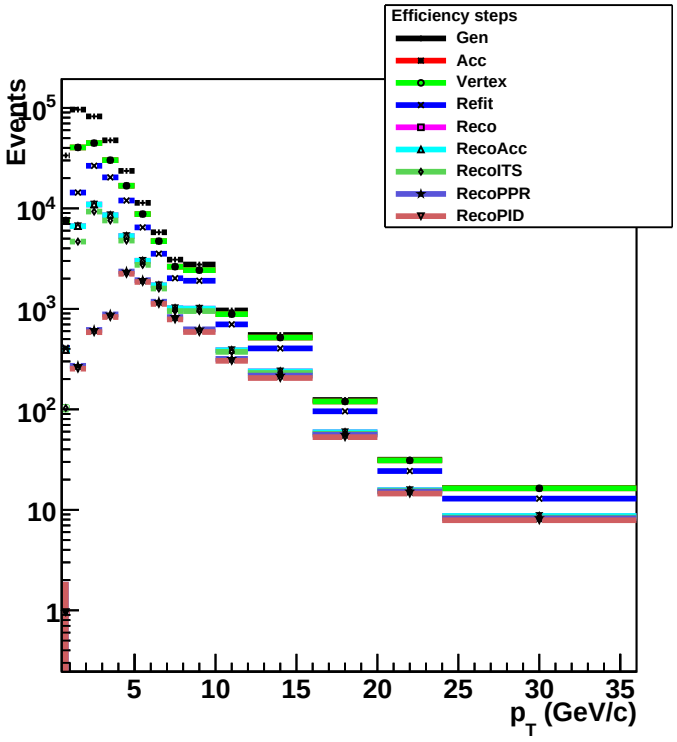

Efficiency relative to first step for each bin:

	Gen	Acc	Vertex	Refit	Reco	RecoAcc	RecoITS	RecoPPR	RecoPID
0.5 - 1	1	0.225	0.225	0.0122	0.0116	0.0116	0.00307	2.86e-05	2.86e-05
1 - 2	1	0.42	0.42	0.149	0.0692	0.0692	0.0486	0.00282	0.00264
2 - 3	1	0.543	0.543	0.322	0.133	0.133	0.113	0.0075	0.00712
3 - 4	1	0.635	0.635	0.428	0.18	0.18	0.159	0.0185	0.0174
4 - 5	1	0.711	0.711	0.507	0.225	0.225	0.203	0.0997	0.0946
5 - 6	1	0.773	0.773	0.57	0.265	0.265	0.241	0.17	0.163
6 - 7	1	0.816	0.816	0.612	0.297	0.297	0.276	0.204	0.194
7 - 8	1	0.851	0.851	0.653	0.329	0.329	0.308	0.268	0.254
8 - 10	1	0.879	0.879	0.689	0.364	0.364	0.344	0.227	0.213
10 - 12	1	0.919	0.919	0.727	0.403	0.403	0.387	0.33	0.315
12 - 16	1	0.943	0.943	0.736	0.435	0.435	0.419	0.394	0.373
16 - 20	1	0.967	0.967	0.772	0.478	0.478	0.461	0.452	0.427
20 - 24	1	0.985	0.985	0.771	0.498	0.498	0.487	0.481	0.46
24 - 36	1	0.995	0.995	0.785	0.528	0.528	0.508	0.5	0.479

Efficiency relative to previous step for each bin:

	Acc	Vertex	Refit	Reco	RecoAcc	RecoITS	RecoPPR	RecoPID
0.5 - 1	0.225	1	0.054	0.952	1	0.264	0.00932	1
1 - 2	0.42	1	0.356	0.463	1	0.702	0.058	0.937
2 - 3	0.543	1	0.594	0.412	1	0.85	0.0664	0.949
3 - 4	0.635	1	0.674	0.421	1	0.885	0.116	0.941
4 - 5	0.711	1	0.713	0.443	1	0.901	0.492	0.949
5 - 6	0.773	1	0.736	0.466	1	0.911	0.705	0.959
6 - 7	0.816	1	0.749	0.486	1	0.928	0.739	0.951
7 - 8	0.851	1	0.767	0.504	1	0.936	0.872	0.948
8 - 10	0.879	1	0.784	0.528	1	0.945	0.658	0.94
10 - 12	0.919	1	0.791	0.554	1	0.961	0.852	0.956
12 - 16	0.943	1	0.78	0.591	1	0.963	0.942	0.947
16 - 20	0.967	1	0.798	0.619	1	0.964	0.98	0.945
20 - 24	0.985	1	0.783	0.646	1	0.978	0.988	0.957
24 - 36	0.995	1	0.789	0.673	1	0.962	0.984	0.958

Pseudo rapidity

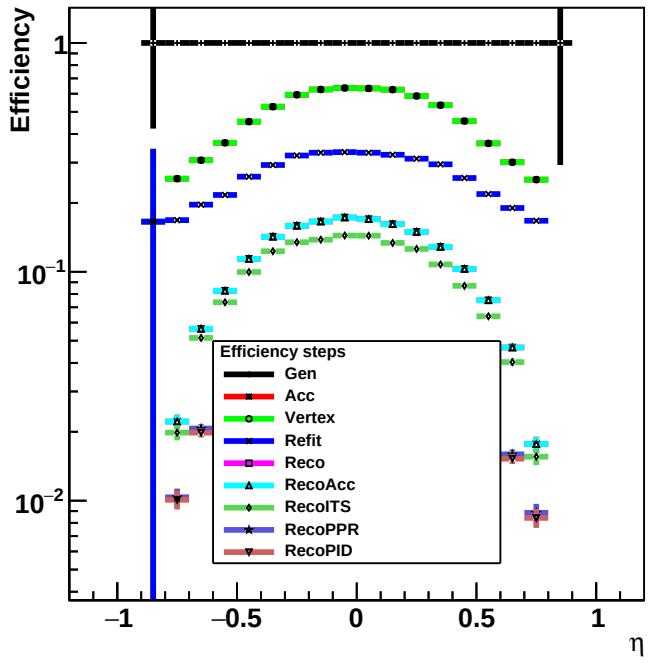

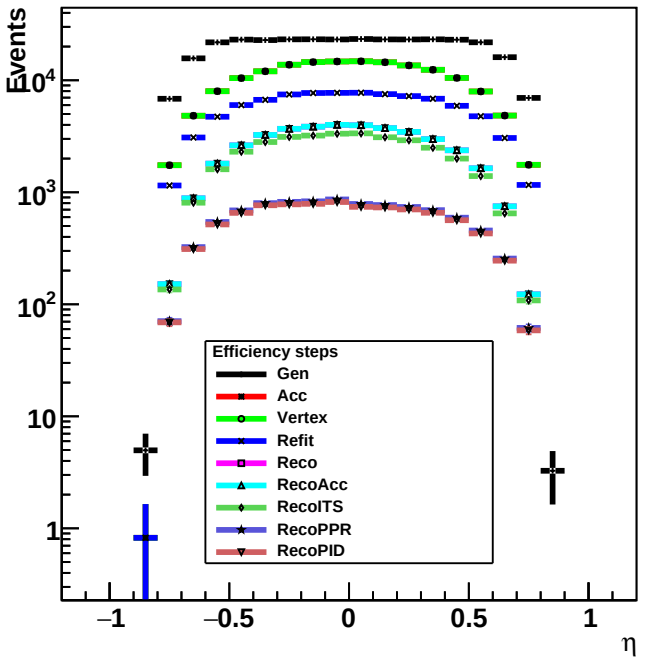

Efficiency relative to first step for each bin:

	Gen	Acc	Vertex	Refit	Reco	RecoAcc	RecoITS	RecoPPR	RecoPID
-1.2 - -1.1	0	0	0	0	0	0	0	0	0
-1.1 - -1	0	0	0	0	0	0	0	0	0
-1 - -0.9	0	0	0	0	0	0	0	0	0
-0.9 - -0.8	1	0.166	0.166	0.166	0	0	0	0	0
-0.8 - -0.7	1	0.255	0.255	0.168	0.0222	0.0222	0.0198	0.0103	0.0101
-0.7 - -0.6	1	0.307	0.307	0.197	0.0564	0.0564	0.0514	0.0207	0.0198
-0.6 - -0.5	1	0.366	0.366	0.217	0.0827	0.0827	0.0736	0.0249	0.0237
-0.5 - -0.4	1	0.453	0.453	0.26	0.114	0.114	0.0998	0.0299	0.0284
-0.4 - -0.3	1	0.527	0.526	0.293	0.142	0.142	0.123	0.035	0.0335
-0.3 - -0.2	1	0.593	0.593	0.322	0.159	0.159	0.135	0.0354	0.0336
-0.2 - -0.1	1	0.626	0.626	0.331	0.166	0.166	0.138	0.0358	0.034
-0.1 - 0	1	0.636	0.636	0.333	0.173	0.173	0.144	0.0373	0.0354
0 - 0.1	1	0.633	0.633	0.331	0.17	0.17	0.144	0.0337	0.0317
0.1 - 0.2	1	0.625	0.625	0.325	0.162	0.162	0.134	0.0332	0.0316
0.2 - 0.3	1	0.586	0.586	0.312	0.149	0.149	0.126	0.032	0.0304
0.3 - 0.4	1	0.535	0.535	0.295	0.129	0.129	0.108	0.0299	0.0283
0.4 - 0.5	1	0.456	0.456	0.257	0.103	0.103	0.0868	0.0258	0.0245
0.5 - 0.6	1	0.364	0.364	0.219	0.0751	0.0751	0.0639	0.0209	0.0197
0.6 - 0.7	1	0.301	0.301	0.19	0.0467	0.0467	0.0403	0.0159	0.0153
0.7 - 0.8	1	0.253	0.253	0.167	0.0177	0.0177	0.0156	0.00885	0.00841
0.8 - 0.9	1	0	0	0	0	0	0	0	0
0.9 - 1	0	0	0	0	0	0	0	0	0
1 - 1.1	0	0	0	0	0	0	0	0	0
1.1 - 1.2	0	0	0	0	0	0	0	0	0

Efficiency relative to previous step for each bin:

	Acc	Vertex	Refit	Reco	RecoAcc	RecoITS	RecoPPR	RecoPID
-1.2 - -1.1	0	0	0	0	0	0	0	0
-1.1 - -1	0	0	0	0	0	0	0	0
-1 - -0.9	0	0	0	0	0	0	0	0
-0.9 - -0.8	0.166	1	1	0	0	0	0	0
-0.8 - -0.7	0.255	1	0.659	0.132	1	0.895	0.522	0.975
-0.7 - -0.6	0.307	1	0.639	0.287	1	0.912	0.402	0.96
-0.6 - -0.5	0.366	1	0.592	0.382	1	0.89	0.339	0.95
-0.5 - -0.4	0.453	1	0.575	0.437	1	0.876	0.299	0.95
-0.4 - -0.3	0.527	1	0.556	0.486	1	0.864	0.285	0.957
-0.3 - -0.2	0.593	1	0.543	0.493	1	0.847	0.263	0.95
-0.2 - -0.1	0.626	1	0.529	0.5	1	0.833	0.259	0.949
-0.1 - 0	0.636	1	0.525	0.518	1	0.834	0.259	0.948
0 - 0.1	0.633	1	0.524	0.513	1	0.846	0.234	0.942
0.1 - 0.2	0.625	1	0.519	0.498	1	0.828	0.248	0.951
0.2 - 0.3	0.586	1	0.532	0.479	1	0.842	0.254	0.95
0.3 - 0.4	0.535	1	0.552	0.436	1	0.838	0.277	0.947
0.4 - 0.5	0.456	1	0.564	0.401	1	0.843	0.297	0.949
0.5 - 0.6	0.364	1	0.601	0.343	1	0.851	0.327	0.941
0.6 - 0.7	0.301	1	0.631	0.246	1	0.864	0.395	0.957
0.7 - 0.8	0.253	1	0.661	0.106	1	0.881	0.569	0.95
0.8 - 0.9	0	0	0	0	0	0	0	0
0.9 - 1	0	0	0	0	0	0	0	0
1 - 1.1	0	0	0	0	0	0	0	0
1.1 - 1.2	0	0	0	0	0	0	0	0

$\cos(\theta^*)$

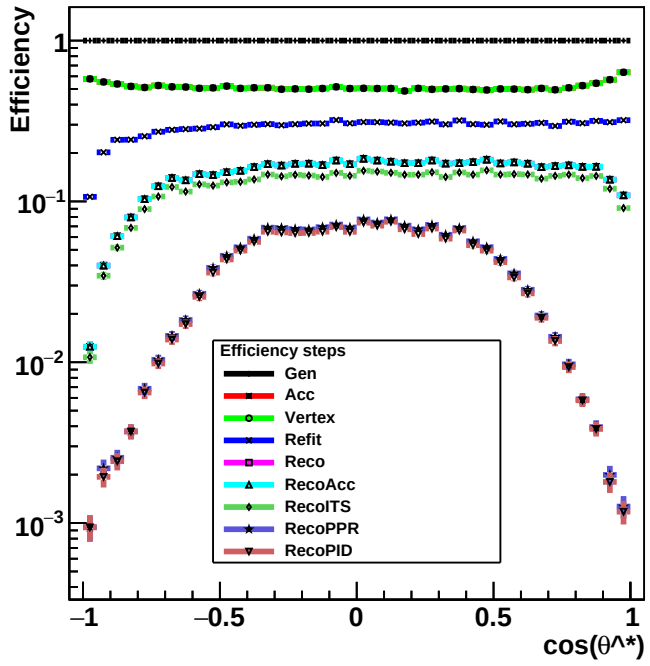

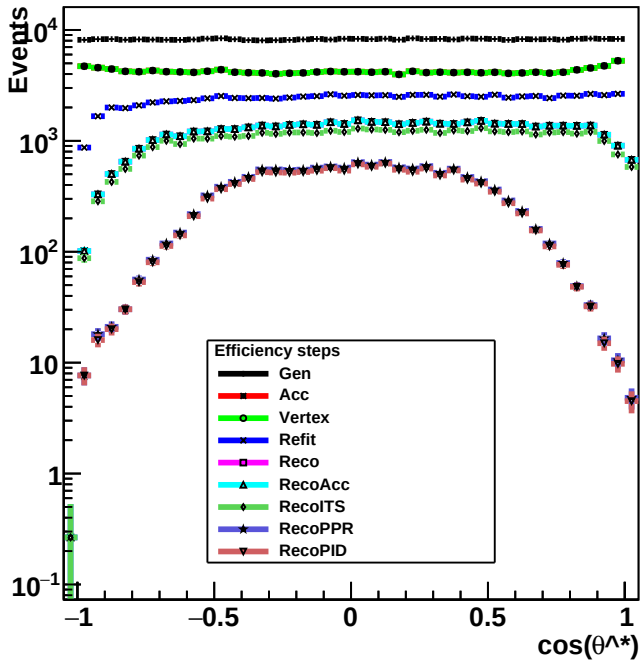

Efficiency relative to first step for each bin:

	Gen	Acc	Vertex	Refit	Reco	RecoAcc	RecoITS	RecoPPR	RecoPID
-1.05 - -1	0	0	0	0	0	0	0	0	0
-1 - -0.95	1	0.578	0.578	0.107	0.0125	0.0125	0.0107	0.000941	0.00094
-0.95 - -0.9	1	0.553	0.553	0.202	0.0399	0.0399	0.0345	0.00219	0.00194
-0.9 - -0.85	1	0.538	0.537	0.242	0.0608	0.0608	0.0516	0.00255	0.00243
-0.85 - -0.8	1	0.519	0.519	0.242	0.0796	0.0796	0.0685	0.00371	0.00371
-0.8 - -0.75	1	0.511	0.511	0.254	0.103	0.103	0.0896	0.00684	0.00648
-0.75 - -0.7	1	0.526	0.526	0.271	0.124	0.124	0.107	0.0104	0.00982
-0.7 - -0.65	1	0.516	0.516	0.279	0.14	0.14	0.123	0.0146	0.0138
-0.65 - -0.6	1	0.514	0.514	0.282	0.135	0.135	0.115	0.0183	0.0173
-0.6 - -0.55	1	0.506	0.505	0.284	0.148	0.148	0.128	0.0266	0.0255
-0.55 - -0.5	1	0.508	0.508	0.29	0.146	0.146	0.125	0.0386	0.0361
-0.5 - -0.45	1	0.521	0.521	0.302	0.152	0.152	0.131	0.0459	0.0436
-0.45 - -0.4	1	0.505	0.505	0.296	0.155	0.155	0.132	0.0519	0.0495
-0.4 - -0.35	1	0.509	0.509	0.3	0.164	0.164	0.137	0.0586	0.056
-0.35 - -0.3	1	0.509	0.509	0.302	0.171	0.171	0.147	0.0687	0.0648
-0.3 - -0.25	1	0.499	0.498	0.298	0.167	0.167	0.143	0.0685	0.0642
-0.25 - -0.2	1	0.501	0.501	0.302	0.171	0.171	0.146	0.0673	0.0635
-0.2 - -0.15	1	0.499	0.499	0.305	0.172	0.172	0.145	0.067	0.0637
-0.15 - -0.1	1	0.504	0.504	0.305	0.168	0.168	0.142	0.0692	0.0648
-0.1 - -0.05	1	0.516	0.516	0.321	0.18	0.18	0.15	0.0718	0.0692
-0.05 - 0	1	0.504	0.503	0.306	0.171	0.171	0.144	0.0689	0.0647
0 - 0.05	1	0.505	0.505	0.312	0.184	0.184	0.155	0.0774	0.0738
0.05 - 0.1	1	0.504	0.503	0.311	0.18	0.18	0.153	0.074	0.0707
0.1 - 0.15	1	0.504	0.504	0.309	0.177	0.177	0.151	0.0774	0.0747
0.15 - 0.2	1	0.486	0.486	0.305	0.173	0.173	0.147	0.0707	0.0671
0.2 - 0.25	1	0.505	0.505	0.309	0.173	0.173	0.147	0.0671	0.0627
0.25 - 0.3	1	0.498	0.498	0.314	0.18	0.18	0.152	0.0714	0.0678
0.3 - 0.35	1	0.501	0.501	0.302	0.172	0.172	0.142	0.0621	0.0587
0.35 - 0.4	1	0.503	0.503	0.319	0.173	0.173	0.151	0.0684	0.0659
0.4 - 0.45	1	0.497	0.497	0.302	0.176	0.176	0.147	0.0565	0.0535
0.45 - 0.5	1	0.493	0.493	0.3	0.182	0.182	0.156	0.052	0.0494
0.5 - 0.55	1	0.501	0.501	0.314	0.172	0.172	0.147	0.0439	0.0419
0.55 - 0.6	1	0.5	0.5	0.302	0.175	0.175	0.148	0.0357	0.0337
0.6 - 0.65	1	0.495	0.495	0.304	0.172	0.172	0.147	0.0282	0.0268
0.65 - 0.7	1	0.505	0.505	0.308	0.164	0.164	0.139	0.0195	0.0189
0.7 - 0.75	1	0.495	0.494	0.295	0.166	0.166	0.144	0.0144	0.0136
0.75 - 0.8	1	0.509	0.509	0.313	0.168	0.168	0.147	0.00971	0.00934
0.8 - 0.85	1	0.525	0.525	0.307	0.164	0.164	0.14	0.00588	0.0058
0.85 - 0.9	1	0.543	0.543	0.317	0.164	0.164	0.144	0.00395	0.00385
0.9 - 0.95	1	0.571	0.571	0.311	0.137	0.137	0.12	0.00199	0.0018
0.95 - 1	1	0.636	0.636	0.32	0.109	0.109	0.0909	0.00127	0.00118
1 - 1.05	0	0	0	0	0	0	0	0	0

Efficiency relative to previous step for each bin:

	Acc	Vertex	Refit	Reco	RecoAcc	RecoITS	RecoPPR	RecoPID
-1.05 - -1	0	0	0	0	0	0	0	0
-1 - -0.95	0.578	1	0.185	0.117	1	0.861	0.0877	1
-0.95 - -0.9	0.553	1	0.365	0.197	1	0.865	0.0634	0.885
-0.9 - -0.85	0.538	1	0.45	0.252	1	0.848	0.0494	0.953
-0.85 - -0.8	0.519	1	0.466	0.329	1	0.861	0.0542	1
-0.8 - -0.75	0.511	0.999	0.497	0.406	1	0.867	0.0763	0.948
-0.75 - -0.7	0.526	1	0.516	0.458	1	0.863	0.0966	0.948
-0.7 - -0.65	0.516	1	0.54	0.502	1	0.878	0.119	0.948
-0.65 - -0.6	0.514	1	0.547	0.481	1	0.851	0.159	0.943
-0.6 - -0.55	0.506	0.999	0.562	0.521	1	0.864	0.209	0.957
-0.55 - -0.5	0.508	1	0.57	0.504	1	0.86	0.308	0.934
-0.5 - -0.45	0.521	1	0.578	0.505	1	0.864	0.349	0.949
-0.45 - -0.4	0.505	1	0.586	0.525	1	0.854	0.392	0.954
-0.4 - -0.35	0.509	1	0.589	0.546	1	0.837	0.428	0.956
-0.35 - -0.3	0.509	1	0.594	0.565	1	0.861	0.468	0.943
-0.3 - -0.25	0.499	0.999	0.597	0.562	1	0.857	0.478	0.937
-0.25 - -0.2	0.501	1	0.603	0.567	1	0.854	0.46	0.943
-0.2 - -0.15	0.499	1	0.612	0.563	1	0.844	0.462	0.951
-0.15 - -0.1	0.504	1	0.606	0.552	1	0.844	0.487	0.937
-0.1 - -0.05	0.516	1	0.622	0.56	1	0.837	0.477	0.964
-0.05 - 0	0.504	0.999	0.608	0.557	1	0.847	0.477	0.939
0 - 0.05	0.505	1	0.617	0.591	1	0.843	0.498	0.954
0.05 - 0.1	0.504	0.999	0.618	0.577	1	0.854	0.482	0.955
0.1 - 0.15	0.504	1	0.613	0.571	1	0.853	0.514	0.965
0.15 - 0.2	0.486	1	0.628	0.566	1	0.848	0.482	0.949
0.2 - 0.25	0.505	0.999	0.612	0.56	1	0.849	0.457	0.934
0.25 - 0.3	0.498	0.999	0.63	0.573	1	0.845	0.471	0.949
0.3 - 0.35	0.501	1	0.602	0.57	1	0.826	0.437	0.946
0.35 - 0.4	0.503	1	0.634	0.543	1	0.874	0.452	0.963
0.4 - 0.45	0.497	0.999	0.609	0.581	1	0.835	0.385	0.946
0.45 - 0.5	0.493	1	0.608	0.606	1	0.859	0.333	0.951
0.5 - 0.55	0.501	0.999	0.627	0.549	1	0.852	0.299	0.954
0.55 - 0.6	0.5	1	0.604	0.579	1	0.845	0.242	0.943
0.6 - 0.65	0.495	1	0.614	0.565	1	0.857	0.192	0.95
0.65 - 0.7	0.505	0.999	0.61	0.531	1	0.848	0.141	0.968
0.7 - 0.75	0.495	1	0.596	0.564	1	0.868	0.0999	0.941
0.75 - 0.8	0.509	1	0.615	0.536	1	0.875	0.0661	0.962
0.8 - 0.85	0.525	1	0.584	0.535	1	0.851	0.0421	0.987
0.85 - 0.9	0.543	1	0.583	0.519	1	0.877	0.0275	0.974
0.9 - 0.95	0.571	1	0.545	0.439	1	0.879	0.0166	0.904
0.95 - 1	0.636	1	0.503	0.341	1	0.834	0.0139	0.929
1 - 1.05	0	0	0	0	0	0	0	0